

Spin-1/2 XXZ chain coupled to two Lindblad baths: Constructing nonequilibrium steady states from equilibrium correlation functions

Tjark Heitmann ,^{1,*} Jonas Richter ,^{2,3} Fengping Jin ,⁴ Sourav Nandy,⁵ Zala Lenarčič ,⁵ Jacek Herbrych ,⁶ Kristel Michelsen ,⁴ Hans De Raedt ,⁷ Jochen Gemmer,¹ and Robin Steinigeweg ,^{1,†}

¹*Department of Mathematics/Computer Science/Physics,*

University of Osnabrück, D-49076 Osnabrück, Germany

²*Department of Physics, Stanford University, Stanford, California 94305, USA*

³*Institut für Theoretische Physik, Leibniz Universität Hannover, 30167 Hannover, Germany*

⁴*Institute for Advanced Simulation, Jülich Supercomputing Centre,*

Forschungszentrum Jülich, D-52425 Jülich, Germany

⁵*Jožef Stefan Institute, SI-1000 Ljubljana, Slovenia*

⁶*Wroclaw University of Science and Technology, 50-370 Wroclaw, Poland*

⁷*Zernike Institute for Advanced Materials, University of Groningen, NL-9747 AG Groningen, Netherlands*

(Dated: November 28, 2023)

State-of-the-art approaches to extract transport coefficients of many-body quantum systems broadly fall into two categories: (i) they target the linear-response regime in terms of equilibrium correlation functions of the closed system; or (ii) they consider an open-system situation typically modeled by a Lindblad equation, where a nonequilibrium steady state emerges from driving the system at its boundaries. While quantitative agreement between (i) and (ii) has been found for selected model and parameter choices, also disagreement has been pointed out in the literature. Studying magnetization transport in the spin-1/2 XXZ chain, we here demonstrate that at weak driving, the nonequilibrium steady state in an open system, including its buildup in time, can remarkably be constructed just on the basis of correlation functions in the closed system. We numerically illustrate this direct correspondence of closed-system and open-system dynamics, and show that it allows the treatment of comparatively large open systems, usually only accessible to matrix product state simulations. We also point out potential pitfalls when extracting transport coefficients from nonequilibrium steady states in finite systems.

Introduction. Our understanding of the properties of many-body quantum systems out of equilibrium has seen remarkable advances in the last decades thanks to various experimental and theoretical breakthroughs [1–5]. Central questions are concerned with the emergence of particular (thermal or nonthermal) steady states in the long-time limit, but also with the (universal) properties of the actual nonequilibrium process towards such states in the course of time [2–5]. Broadly speaking, these and related questions are usually studied in two different scenarios: (i) the system of interest is perfectly isolated from its environment and evolves unitarily in time; (ii) the system's time evolution is nonunitary due to an explicit coupling to an external bath which can affect the dynamics (see, e.g., Ref. [6–8]).

In systems with a global conservation law, a fundamental role is played by transport processes [9]. Quantum transport is also a prime example of a research question that is explored both from a closed-system and an open-system perspective. In closed systems, a widely used approach is linear response theory, where the Kubo formula allows for the extraction of transport coefficients from equilibrium correlation functions, which can be studied in the time or frequency domain and in real or momentum space [9]. While nonintegrable systems are expected

to exhibit normal diffusion [10–12], the concrete calculation of diffusion constants for specific models turns out to be a hard task in practice. This difficulty has been one of the motivations for the development of sophisticated numerical methods [13–27]. Moreover, some classes of models can generically feature anomalous subdiffusion or superdiffusion in certain parameter regimes [2, 28–41].

In contrast, when studying transport in an open-system setting, the model of interest is often coupled at its edges to two reservoirs, e.g., at different temperatures or chemical potentials, leading to a nonequilibrium steady state in the long-time limit. Then, the profile and current of this steady state yield information on the transport behavior [42–45]. A popular description of such an open system is provided by the Lindblad quantum master equation [6], not least since it allows for efficient numerical simulations based on matrix product states, giving access to comparatively large system sizes [39, 46–51]. While quantitative agreement of transport coefficients according to the Lindblad description with those from closed-system approaches has been found for selected models and parameter regimes [52–54], also disagreement has been pointed out in the literature [55], and there is no proof that both approaches have to agree [9, 55–58].

From a physical perspective, computed transport coefficients for a given system should of course be independent of the method employed. In fact, some of us have recently shown that the dynamics of closed and

* tjark.heitmann@uos.de

† rsteinig@uos.de

open systems can be connected with each other in a certain simple setting. Specifically, Ref. [54] considered an initially homogeneous system coupled locally to a single Lindblad bath, which induces a net magnetization into the system. Remarkably, it was shown that if the Lindblad driving is weak, the flow of the magnetization in the open system, i.e., the broadening of the nonequilibrium density profile, can be described by an appropriate superposition of equilibrium correlation functions in the closed system. Building on this result, we here go beyond Ref. [54] in a crucial point and explore the more common situation of two Lindblad baths inducing a nonequilibrium steady state. Considering magnetization transport in the paradigmatic spin-1/2 XXZ chain as an example, we demonstrate that the steady state in the open system can be constructed on the basis of correlation functions in the closed system. We support our analytical results by large-scale numerical simulations and show that our scheme enables efficient unravelings of Lindblad equations for systems with up to 36 sites, which are usually only accessible with matrix product state techniques.

Closed System. We consider the one-dimensional XXZ model, which is described by the Hamiltonian

$$H = J \sum_{r=1}^N (S_r^x S_{r+1}^x + S_r^y S_{r+1}^y + \Delta S_r^z S_{r+1}^z), \quad (1)$$

where S_r^j ($j = x, y, z$) are spin-1/2 operators at site r , $J > 0$ is the antiferromagnetic coupling constant, and Δ denotes the anisotropy in the z direction. Moreover, N is the number of sites and we employ periodic boundary conditions, $S_{N+1}^j \equiv S_1^j$. The XXZ chain conserves the global magnetization, $[H, \sum_r S_r^z] = 0$, and we will particularly focus on the regime $\Delta > 1$, where it is well-established that spin transport is diffusive [9]. This diffusive transport behavior can, for instance, be seen in the Gaussian shape of the infinite-temperature spin-spin correlation function at $\Delta = 1.5$ [59], see Fig. 1(a),

$$\langle S_r^z(t) S_{r'}^z(0) \rangle_{\text{eq}} = \frac{\text{tr}[e^{iHt} S_r^z e^{-iHt} S_{r'}^z]}{2N}. \quad (2)$$

The root-mean-squared displacement of the above grows as $\Sigma(t) \propto \sqrt{t}$, see Fig. 1(b), where $\Sigma^2(t) = \sum_r (r - r')^2 C_{rr'}(t) - [\sum_r (r - r') C_{rr'}(t)]^2$ and $C_{rr'}(t) = 4 \langle S_r^z(t) S_{r'}^z \rangle_{\text{eq}}$. Moreover, a diffusion coefficient can be defined as $2D(t) = \frac{d}{dt} \Sigma^2(t)$ [60]. As shown in Fig. 1(b), $D(t)$ takes on a constant value $D/J \approx 0.6$ for $tJ \lesssim 10$, which is approximately independent of time (and system size [59, 61]) and consistent with other results in the literature [51, 62–64].

In the following, we will show that the equilibrium correlation function $\langle S_r^z(t) S_{r'}^z(0) \rangle_{\text{eq}}$ in Eq. (2) is not only central to transport in the closed system, but can remarkably be used to predict the buildup of a nonequilibrium steady state in an open-system situation where the spin chain is weakly driven by two Lindblad baths. While we focus on the integrable XXZ chain as a concrete

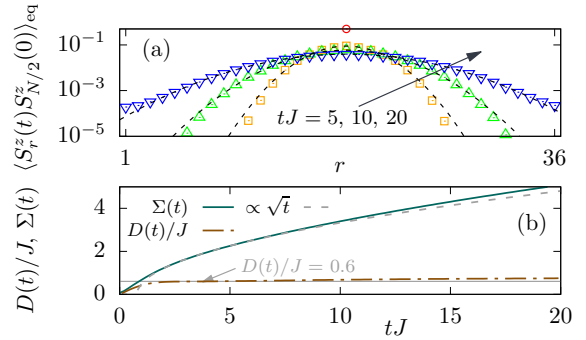


FIG. 1. (a) Infinite-temperature correlation function $\langle S_r^z(t) S_{N/2}^z(0) \rangle_{\text{eq}}$ for $N = 36$ and $\Delta = 1.5$. The dashed curves indicate Gaussians, see also [59]. (b) Diffusive growth of root-mean-squared displacement $\Sigma(t) \propto \sqrt{t}$. A diffusion constant $D/J \approx 0.6$ can be extracted from the approximately constant plateau of $2D(t) = \frac{d}{dt} \Sigma^2(t)$ at $tJ \lesssim 10$. For longer times, finite-size effects become relevant.

example due to its interesting transport properties, we expect our conceptual findings to apply to a wider range of models. In particular, while our derivation [54, 65] is largely model-independent, it implicitly assumes sufficiently fast local equilibration, which should be even better fulfilled in nonintegrable chaotic systems.

Open System. Let us consider a scenario, where the XXZ chain is explicitly coupled to an environment. We describe this setting with a Lindblad equation,

$$\dot{\rho}(t) = \mathcal{L} \rho(t) = i[\rho(t), H] + \mathcal{D} \rho(t), \quad (3)$$

which consists of a coherent time evolution of the density matrix ρ with respect to H and an incoherent damping term,

$$\mathcal{D} \rho(t) = \sum_j \alpha_j \left(L_j \rho(t) L_j^\dagger - \frac{1}{2} \{ \rho(t), L_j^\dagger L_j \} \right), \quad (4)$$

with non-negative rates α_j , Lindblad operators L_j , and the anticommutator $\{\bullet, \bullet\}$. While the derivation of this equation can be a subtle task for a given microscopic model [43, 66], it is the most general form of a time-local quantum master equation, which maps any density matrix to a density matrix, i.e., which preserves trace, hermiticity, and positivity [6]. Here, we choose [9]

$$L_1 = S_{B_1}^+, \quad \alpha_1 = \gamma(1 + \mu) \quad (5)$$

$$L_2 = L_1^\dagger = S_{B_1}^-, \quad \alpha_2 = \gamma(1 - \mu) \quad (6)$$

$$L_3 = S_{B_2}^+, \quad \alpha_3 = \gamma(1 - \mu) \quad (7)$$

$$L_4 = L_3^\dagger = S_{B_2}^-, \quad \alpha_4 = \gamma(1 + \mu), \quad (8)$$

where γ is the system-bath coupling and μ is the driving strength. L_1 and L_2 are local Lindblad operators at site B_1 and flip a spin up and down, respectively. L_3 and L_4 act similarly on another site B_2 . In the following, we set $B_1 = 1$ and $B_2 = N/2 + 1$. Note that we still

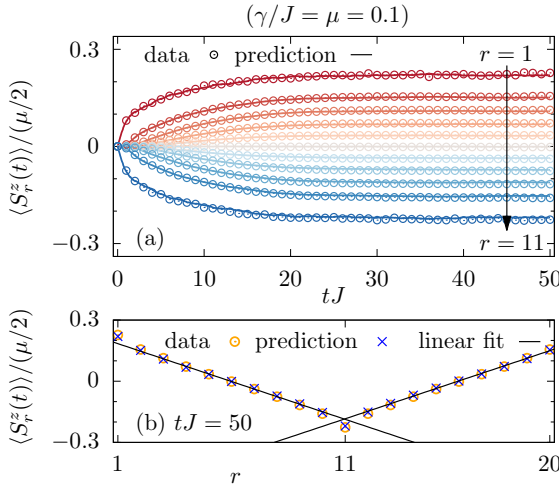


FIG. 2. Open-system dynamics for the spin-1/2 XXZ chain coupled to two Lindblad baths, as obtained for anisotropy $\Delta = 1.5$, $N = 20$ sites (with periodic boundary conditions), small coupling $\gamma/J = 0.1$, and weak driving $\mu = 0.1$. Numerical results from the full stochastic unraveling (data) are compared to the prediction based on closed-system correlation functions [cf. Eq. (20)]. (a) Time evolution of the local magnetization $\langle S_r^z(t) \rangle$ for different sites r . (b) Site dependence of the steady state at $tJ = 50$.

consider periodic boundary conditions. However, our approach can also generally be applied to open boundaries with the two baths at the system's edges $B_1 = 1$ and $B_2 = N$, and we present results for this setting in [65]. For $\mu > 0$, the first (second) bath induces a net polarization of $\mu/2$ ($-\mu/2$), leading to a steady state in the long-time limit with a characteristic density profile and a constant current. Note that, while the Lindblad modeling (3) - (8) is standard in the context of transport in quantum lattice models [9], there exist other approaches to open-system dynamics which can also address potential non-Markovian effects [67].

In addition to the long-time limit, we are interested in the temporal buildup of the steady state. Thus, we study the time evolution of local densities

$$\langle S_r^z(t) \rangle = \text{tr}[\rho(t) S_r^z], \quad (9)$$

which depends on the parameters of the system H , but also on the bath parameters γ and μ . As an initial state, we here consider a homogeneous situation with $\rho(0) \propto \mathbb{1}$ being the infinite-temperature ensemble.

Quantum-trajectory approach. One possibility to solve the Lindblad equation is given by the concept of stochastic unraveling, which relies on pure states $|\psi\rangle$ rather than density matrices [68, 69]. It consists of an alternating sequence of stochastic jumps with one of the Lindblad operators and deterministic evolutions governed by an effective Hamiltonian $H_{\text{eff}} = H - \frac{i}{2} \sum_j \alpha_j L_j^\dagger L_j$. For our choice of Lindblad operators,

$$H_{\text{eff}} = H - i\gamma + i\gamma\mu(n_{B_1} - n_{B_2}), \quad (10)$$

with $n_r = S_r^+ S_r^- = S_r^z + \mathbb{1}/2$. For weak driving $\mu \ll 1$, the time scale on which the last term in Eq. 10 affects the dynamics is much longer than the typical time scale between jumps. Thus, the effective Hamiltonian can be approximated as

$$H_{\text{eff}} \approx H - i\gamma \quad (11)$$

and the time evolution of a pure state reads

$$|\psi(t)\rangle \approx e^{-\gamma t} e^{-iHt} |\psi(0)\rangle, \quad (12)$$

i.e., apart from the scalar damping term, the dynamics is generated by the closed system H only. The approximation in Eq. (12) is one of the main ingredients to establish a correspondence between the dynamics of the isolated and the weakly-driven XXZ chain below. For larger values of μ , the effective Hamiltonian generating the dynamics of $|\psi(t)\rangle$ also involves the two operators n_{B_1} and n_{B_2} , cf. Eq. (10).

Naturally, since H_{eff} is a non-Hermitian operator, the norm of a pure state is not conserved as a function of time. As a consequence, for a given ε drawn at random from a uniform distribution $[0, 1]$, there is a time, where the condition $\|\psi(t)\|^2 > \varepsilon$ is first violated. At this time, a jump with one of the Lindblad operators occurs and the new and normalized pure state reads

$$|\psi'(t)\rangle = \frac{L_j |\psi(t)\rangle}{\|L_j |\psi(t)\rangle\|}, \quad (13)$$

where the specific jump is chosen with probability

$$p_j = \frac{\alpha_j \|L_j |\psi(t)\rangle\|^2}{\sum_j \alpha_j \|L_j |\psi(t)\rangle\|^2}. \quad (14)$$

After this jump, the next deterministic evolution takes place. This sequence of stochastic jumps and deterministic evolutions leads to a particular trajectory $|\psi_T(t)\rangle$. The time-dependent density matrix according to the Lindblad equation can eventually be approximated by the average over different trajectories T . Thus, expectation values read

$$\langle S_r^z(t) \rangle \approx \frac{1}{T_{\text{max}}} \sum_{T=1}^{T_{\text{max}}} \frac{\langle \psi_T(t) | S_r^z | \psi_T(t) \rangle}{\|\psi_T(t)\|^2}, \quad (15)$$

where T_{max} is the number of trajectories.

In order to mimic the homogeneous state $\rho(0) \propto \mathbb{1}$, we use random pure states as initial condition for the stochastic unraveling,

$$|\psi(0)\rangle \propto \sum_j c_j |\phi_j\rangle, \quad (16)$$

where the real and imaginary parts of the coefficients c_j in some given basis $|\phi_j\rangle$ are drawn at random according to a Gaussian probability distribution with zero mean. Crucially, by exploiting the concept of quantum typicality

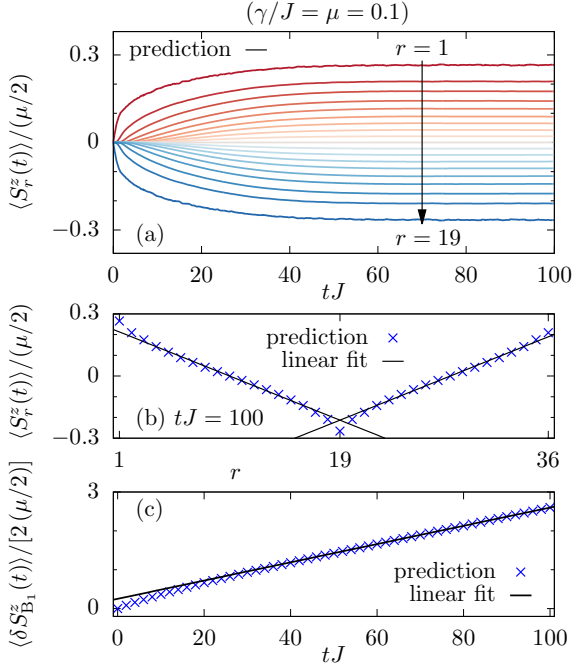


FIG. 3. [(a) and (b)] Analogous data as in Fig. 2, but now for $N = 36$ sites, for which stochastic unraveling is unfeasible. (c) Magnetization injected by the first bath as a function of time, see also [65]. A diffusion constant $D/J \approx 0.99$ [76] can be extracted from the slopes in (b) and (c).

[59, 70–75], expectation values $\langle \psi | \bullet | \psi \rangle$ of local observables evaluated within such random states can be related to infinite-temperature averages $\text{tr}[\bullet]/2^N$. This is used in the following to connect the equilibrium correlation functions $\langle S_r^z(t) S_r^z(0) \rangle_{\text{eq}}$ [Eq. (2)] to the dynamics $\langle S_r^z(t) \rangle$ in the open system [Eq. (9)].

Constructing steady states from correlation functions. In Ref. [54], it was demonstrated that individual quantum trajectories of the open system can be described by closed-system equilibrium correlation functions if the driving by the Lindblad bath is weak. We here build on this result and apply it to the case of two Lindblad baths leading to a nonequilibrium steady state. While we relegate details of the derivation to the supplemental material [65], we find that for small coupling γ and weak driving μ , the local magnetization dynamics within a single trajectory T can be approximated as $d_{r,T}(t) \approx \langle \psi_T(t) | S_r^z | \psi_T(t) \rangle / \| \psi_T(t) \|^2$, where

$$d_{r,T}(t) = 2\mu \sum_j A_j \Theta(t - \tau_j) \mathcal{C}_r(t - \tau_j) \quad (17)$$

with $\mathcal{C}_r(t) \equiv \langle S_r^z(t) S_{B_1}^z(0) \rangle_{\text{eq}} - \langle S_r^z(t) S_{B_2}^z(0) \rangle_{\text{eq}}$. Here, $\langle \bullet \rangle_{\text{eq}} = \text{tr}[\bullet]/2^N$ denotes the infinite-temperature ensemble, $\Theta(t)$ is the Heavyside function, and the sum runs over the jump times τ_j of the particular trajectory T .

Moreover, the amplitudes A_j in Eq. (17) read

$$A_j = \frac{a_j - d_{B_1,T}(\tau_j - 0^+)}{\mu} \quad (18)$$

$$\text{with } a_j = \frac{\mu - 2 d_{B_1,T}(\tau_j - 0^+)}{2 - 4\mu d_{B_1,T}(\tau_j - 0^+)}, \quad (19)$$

where $A_j \rightarrow 1/2$ for $d_{B_1,T}(\tau_j - 0^+) \rightarrow 0$. Note that, due to the symmetry $d_{B_1,T}(\tau_j - 0^+) = -d_{B_2,T}(\tau_j - 0^+)$, only B_1 enters the above expressions. Equation (17) is the main result of this Letter. It predicts the magnetization dynamics in the open system by suitably superimposing equilibrium correlation functions of the closed system involving the two bath sites B_1 and B_2 . In particular, from Eq. (17), the trajectory-averaged magnetization dynamics follows as

$$\langle S_r^z(t) \rangle \approx \frac{1}{T_{\text{max}}} \sum_{T=1}^{T_{\text{max}}} d_{r,T}(t), \quad (20)$$

where each $d_{r,T}(t)$ is evaluated for a different sequence (τ_1, τ_2, \dots) of τ_j . Given the exponential damping in Eq. (12), the τ_j can be generated as $\tau_{j+1} = \tau_j - \ln \varepsilon_{j+1}/2\gamma$, where ε_{j+1} are random numbers drawn from a box distribution $[0, 1]$. If the correlation functions $\langle S_r^z(t) S_{B_1}^z(0) \rangle_{\text{eq}}$ and $\langle S_r^z(t) S_{B_2}^z(0) \rangle_{\text{eq}}$ are known, it is thus straightforward to evaluate Eq. (20) for a large number of sequences.

Numerical Illustration. We now test our theoretical prediction and its accuracy for a specific example, namely the spin-1/2 XXZ chain with $\Delta = 1.5$, $N = 20$, and periodic boundary conditions. The baths are located at $B_1 = 1$ and $B_2 = 11$ and we focus on small coupling $\gamma/J = 0.1$ and weak driving $\mu = 0.1$. Additional data for other values of Δ , γ , and μ , as well as for open boundary conditions can be found in [65].

Our theoretical prediction (20) is carried out numerically for $\mathcal{O}(10^4 - 10^5)$ different sequences of jump times, which turns out to be sufficient to obtain negligibly small statistical errors. For comparison, we simulate the exact dynamics of the open system by performing a stochastic unraveling of the Lindblad equation. We stress that while (20) is derived in the limit of weak driving, cf. Eq. (12), the stochastic unraveling is here performed for the full H_{eff} in Eq. (10).

In Fig. 2, we depict the outcome of the comparison. In Fig. 2(a), we show the time evolution of the local magnetization $\langle S_r^z(t) \rangle$ for different sites r . The site dependence of the steady-state profile is depicted in Fig. 2(b) and is well described by a linear function, except for the sites located exactly at the bath contacts. Importantly, we observe a remarkably good agreement between our prediction (20) and the exact open-system dynamics for all times up to $tJ = 50$, where the steady-state profile is already established. This confirms our main result (17). We also note that for larger values of γ and μ , deviations are expected to become more pronounced, see [65].

For $N \gg 20$, stochastic unraveling cannot be carried out, since the required average over many trajectories

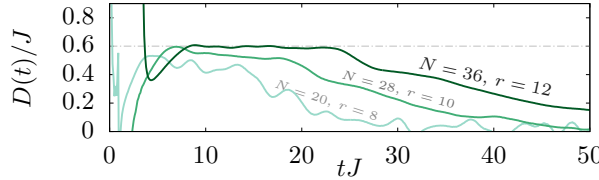


FIG. 4. Diffusion coefficient $D(t) = \partial_t \langle S_r^z(t) \rangle / \nabla^2 \langle S_r^z(t) \rangle$ based on our prediction for the dynamics of the weakly-driven open system in Fig. 3. Data is obtained at lattice site $r = 12$ and the approximately constant plateau for $tJ \lesssim 25$ is consistent with the transport behavior of the isolated XXZ chain in Fig. 1. Similar data for predictions in smaller systems with $N = 20$ and $N = 28$ are shown for comparison.

becomes unfeasible. In contrast, our theoretical prediction (20) can be evaluated for larger system sizes, since only the equilibrium correlation functions are needed in Eq. (17). In particular, by relying on quantum typicality [24, 26], we simulate these correlation functions for up to $N = 36$ lattice sites on Jülich’s “JUWELS” supercomputer. As shown in Figs. 3(a) and 3(b), we are thus able to describe the buildup of a nonequilibrium steady state in a $N = 36$ XXZ chain weakly driven by Lindblad baths at sites $B_1 = 1$ and $B_2 = 19$. Open-system simulations for such system sizes are typically only accessible with matrix product state techniques, which are in turn usually restricted to open boundary conditions.

On the extraction of transport coefficients. In the nonequilibrium steady state, the diffusion constant can be calculated as $D = -\langle j_r \rangle / \nabla \langle S_r \rangle$ for some site r in the bulk away from the bath sites. Here, j_r is the local spin-current operator. Its expectation value can be expressed as $\langle j_r \rangle = \frac{d}{dt} \langle \delta S_{B_1}^z(t) \rangle / 2$, where $\langle \delta S_{B_1}^z(t) \rangle$ is the magnetization injected by the first bath (see [65] for more details), and the factor 1/2 takes into account that magnetization can flow to the left and to the right of this bath, due to periodic boundary conditions. As shown in Fig. 3(c), $\langle \delta S_{B_1}^z(t) \rangle$ grows linearly in time (i.e., a constant $\langle j_r \rangle$) and we can thus evaluate the diffusion constant in the steady state as the ratio of the slopes in Figs. 3(b) and 3(c). In this way, we obtain a value $D/J \approx 0.99$ which differs notably from what we found earlier in the context of Fig. 1.

This discrepancy may be explained by finite-size effects. Specifically, as also apparent in Fig. 1(a), the equilibrium correlation function $\langle S_r^z(t) S_r^z(0) \rangle_{\text{eq}}$ is affected by finite-size effects already at $tJ \sim 20$, where the broadening of the density profile has explored the full system. These effects then likely translate into the steady state in the weakly-driven open system and its finite- N estimate of the diffusion constant. Such finite-size effects demonstrate that care must be taken when extracting transport properties both in closed and open systems. Importantly, we stress that the main conceptual result of our work, i.e., establishing a connection between weakly-driven Lindblad dynamics and closed quantum systems, remains unabated. In the supplemental material [65],

we provide more details on this issue: Specifically, one can assume an ideal situation where the closed system behaves perfectly diffusive without finite-size corrections (in contrast to Fig. 1), in which case the equilibrium correlation functions $\langle S_r^z(t) S_{r'}^z(0) \rangle_{\text{eq}}$ follow analytically as damped modified Bessel functions [65]. Using this idealized Ansatz, we find that the nonequilibrium steady state indeed yields the same diffusion constant as the closed system.

We note that one can extract a diffusion coefficient also from the finite-time dynamics of the open system, even before the steady state is established, via $D(t) = \partial_t \langle S_r^z(t) \rangle / \nabla^2 \langle S_r^z(t) \rangle$, where $\nabla^2 \langle S_r^z(t) \rangle = \langle S_{r-1}^z(t) \rangle - 2\langle S_r^z(t) \rangle + \langle S_{r+1}^z(t) \rangle$. We are able to find a $D(t)$ in Fig. 4 that exhibits an approximately constant plateau $D/J \approx 0.6$ for $tJ \lesssim 25$ (while at longer t the behavior becomes uncontrolled due to dividing two small numbers), consistent with our analysis of the closed system in Fig. 1.

Conclusion. Considering the example of magnetization transport in the spin-1/2 XXZ chain, we have connected linear response theory to the dynamics in an open quantum system driven by two Lindblad baths. Specifically, building on Ref. [54], we have shown that, at weak driving, the nonequilibrium steady state and its buildup in time can be constructed by suitably superimposing equilibrium correlation functions of the closed system.

Conceptually, our results for a specific model might reflect the natural expectation that transport coefficients obtained from closed-system and open-system approaches should agree with each other, at least if the driving is sufficiently weak. While we have presented data for systems with periodic boundary conditions, we provide additional results in [65], where we consider the more common case of open boundaries with Lindblad driving at the edge spins. In particular, we find that our main result (20) works convincingly also in this case and is in good agreement with state-of-the-art simulations based on time-evolving block decimation [47, 48]. From a practical perspective, our results enable the treatment of quite large open systems, which are usually not accessible by full stochastic unraveling. It would be an interesting attempt to generalize our setting to other jump operators, e.g., dephasing noise with $L_j = S_j^z$, and other questions beyond quantum transport.

Acknowledgments. We sincerely thank J. Wang for fruitful discussions. Our research has been funded by the Deutsche Forschungsgemeinschaft (DFG), projects 397107022 (GE 1657/3-2), 397300368 (MI 1772/4-2), and 397067869 (STE 2243/3-2), within DFG Research Unit FOR 2692, grant no. 355031190. J.R. acknowledges funding from the European Union’s Horizon Europe research and innovation programme, Marie Skłodowska-Curie grant no. 101060162, and the Packard Foundation through a Packard Fellowship in Science and Engineering. We gratefully acknowledge the Gauss Centre for Supercomputing e.V. for funding this project by providing computing time on the GCS Supercomputer JUWELS

[77] at Jülich Supercomputing Centre (JSC). Z. L. and S. N. acknowledge support by the projects J1-2463 and P1-0044 program of the Slovenian Research Agency, EU via QuantERA grant T-NiSQ, and also computing time for the TEBD calculations at the supercomputer Vega at

the Institute of Information Science (IZUM) in Maribor, Slovenia. We also acknowledge computing time at the HPC3 at University Osnabrück, which has been funded by the DFG, grant no. 456666331.

[1] I. Bloch, J. Dalibard, and W. Zwerger, *Many-body physics with ultracold gases*, *Rev. Mod. Phys.* **80**, 885 (2008).

[2] D. A. Abanin, E. Altman, I. Bloch, and M. Serbyn, *Colloquium: Many-body localization, thermalization, and entanglement*, *Rev. Mod. Phys.* **91**, 021001 (2019).

[3] A. Polkovnikov, K. Sengupta, A. Silva, and M. Vengalattore, *Colloquium: Nonequilibrium dynamics of closed interacting quantum systems*, *Rev. Mod. Phys.* **83**, 863 (2011).

[4] J. Eisert, M. Friesdorf, and C. Gogolin, *Quantum many-body systems out of equilibrium*, *Nat. Phys.* **11**, 124 (2015).

[5] L. D’Alessio, Y. Kafri, A. Polkovnikov, and M. Rigol, *From quantum chaos and eigenstate thermalization to statistical mechanics and thermodynamics*, *Adv. Phys.* **65**, 239 (2016).

[6] H.-P. Breuer and F. Petruccione, *The Theory of Open Quantum Systems* (Oxford University Press, 2007).

[7] F. Lange, Z. Lenarčič, and A. Rosch, *Time-dependent generalized Gibbs ensembles in open quantum systems*, *Phys. Rev. B* **97**, 165138 (2018).

[8] A. Rubio-Abadal, J.-y. Choi, J. Zeiher, S. Hollerith, J. Rui, I. Bloch, and C. Gross, *Many-Body Delocalization in the Presence of a Quantum Bath*, *Phys. Rev. X* **9**, 041014 (2019).

[9] B. Bertini, F. Heidrich-Meisner, C. Karrasch, T. Prosen, R. Steinigeweg, and M. Žnidarič, *Finite-temperature transport in one-dimensional quantum lattice models*, *Rev. Mod. Phys.* **93**, 025003 (2021).

[10] J. Lux, J. Müller, A. Mitra, and A. Rosch, *Hydrodynamic long-time tails after a quantum quench*, *Phys. Rev. A* **89**, 053608 (2014).

[11] A. Bohrdt, C. B. Mendl, M. Endres, and M. Knap, *Scrambling and thermalization in a diffusive quantum many-body system*, *New J. Phys.* **19**, 063001 (2017).

[12] J. Richter, F. Jin, H. De Raedt, K. Michielsen, J. Gemmer, and R. Steinigeweg, *Real-time dynamics of typical and untypical states in nonintegrable systems*, *Phys. Rev. B* **97**, 174430 (2018).

[13] M. W. Long, P. Prelovšek, S. El Shawish, J. Karadamoglou, and X. Zotos, *Finite-temperature dynamical correlations using the microcanonical ensemble and the Lanczos algorithm*, *Phys. Rev. B* **68**, 235106 (2003).

[14] F. Heidrich-Meisner, A. Honecker, and W. Brenig, *Transport in quasi one-dimensional spin-1/2 systems*, *Eur. Phys. J. Spec. Top.* **151**, 135 (2007).

[15] S. Grossjohann and W. Brenig, *Hydrodynamic limit for the spin dynamics of the Heisenberg chain from quantum Monte Carlo calculations*, *Phys. Rev. B* **81**, 012404 (2010).

[16] C. Karrasch, J. H. Bardarson, and J. E. Moore, *Finite-Temperature Dynamical Density Matrix Renormalization Group and the Drude Weight of Spin-1/2 Chains*, *Phys. Rev. Lett.* **108**, 227206 (2012).

[17] T. A. Elsayed and B. V. Fine, *Regression Relation for Pure Quantum States and Its Implications for Efficient Computing*, *Phys. Rev. Lett.* **110**, 070404 (2013).

[18] R. Steinigeweg, J. Gemmer, and W. Brenig, *Spin-Current Autocorrelations from Single Pure-State Propagation*, *Phys. Rev. Lett.* **112**, 120601 (2014).

[19] E. Leviatan, F. Pollmann, J. H. Bardarson, D. A. Huse, and E. Altman, *Quantum thermalization dynamics with Matrix-Product States*, *arXiv:1702.08894*.

[20] T. Rakovszky, F. Pollmann, and C. W. von Keyserlingk, *Diffusive Hydrodynamics of Out-of-Time-Ordered Correlators with Charge Conservation*, *Phys. Rev. X* **8**, 031058 (2018).

[21] C. D. White, M. Zaletel, R. S. K. Mong, and G. Refael, *Quantum dynamics of thermalizing systems*, *Phys. Rev. B* **97**, 035127 (2018).

[22] J. Wurtz, A. Polkovnikov, and D. Sels, *Cluster truncated Wigner approximation in strongly interacting systems*, *Ann. Phys. (NY)* **395**, 341 (2018).

[23] J. Richter and R. Steinigeweg, *Combining dynamical quantum typicality and numerical linked cluster expansions*, *Phys. Rev. B* **99**, 094419 (2019).

[24] T. Heitmann, J. Richter, D. Schubert, and R. Steinigeweg, *Selected applications of typicality to real-time dynamics of quantum many-body systems*, *Z. Naturforsch. A* **75**, 421 (2020).

[25] B. Ye, F. Machado, C. D. White, R. S. K. Mong, and N. Y. Yao, *Emergent Hydrodynamics in Nonequilibrium Quantum Systems*, *Phys. Rev. Lett.* **125**, 030601 (2020).

[26] F. Jin, D. Willsch, M. Willsch, H. Lagemann, K. Michielsen, and H. De Raedt, *Random State Technology*, *J. Phys. Soc. Jpn.* **90**, 012001 (2021).

[27] T. Rakovszky, C. W. von Keyserlingk, and F. Pollmann, *Dissipation-assisted operator evolution method for capturing hydrodynamic transport*, *Phys. Rev. B* **105**, 075131 (2022).

[28] R. M. Nandkishore and D. A. Huse, *Many-Body Localization and Thermalization in Quantum Statistical Mechanics*, *Annu. Rev. Condens. Matter Phys.* **6**, 15 (2015).

[29] M. Ljubotina, M. Žnidarič, and T. Prosen, *Spin diffusion from an inhomogeneous quench in an integrable system*, *Nat. Commun.* **8**, 16117 (2017).

[30] D. J. Luitz and Y. B. Lev, *The ergodic side of the many-body localization transition*, *Ann. Phys.* **529**, 1600350 (2017).

[31] S. Gopalakrishnan and R. Vasseur, *Kinetic Theory of Spin Diffusion and Superdiffusion in XXZ Spin Chains*, *Phys. Rev. Lett.* **122**, 127202 (2019).

[32] B. Kloss and Y. Bar Lev, *Spin transport in a long-range-interacting spin chain*, *Phys. Rev. A* **99**, 032114 (2019).

[33] M. Ljubotina, M. Žnidarič, and T. Prosen, *Kardar-Parisi-Zhang Physics in the Quantum Heisenberg Mag-*

net, *Phys. Rev. Lett.* **122**, 210602 (2019).

[34] T. Heitmann, J. Richter, T. Dahm, and R. Steinigeweg, *Density dynamics in the mass-imbalanced Hubbard chain*, *Phys. Rev. B* **102**, 045137 (2020).

[35] A. Schuckert, I. Lovas, and M. Knap, *Nonlocal emergent hydrodynamics in a long-range quantum spin system*, *Phys. Rev. B* **101**, 020416(R) (2020).

[36] V. B. Bulchandani, S. Gopalakrishnan, and E. Ilievski, *Superdiffusion in spin chains*, *J. Stat. Mech.* **2021**, 084001 (2021).

[37] M. Serbyn, D. A. Abanin, and Z. Papić, *Quantum many-body scars and weak breaking of ergodicity*, *Nat. Phys.* **17**, 675 (2021).

[38] H. Singh, B. A. Ware, R. Vasseur, and A. J. Friedman, *Subdiffusion and Many-Body Quantum Chaos with Kinetic Constraints*, *Phys. Rev. Lett.* **127**, 230602 (2021).

[39] S. Nandy, Z. Lenarčič, E. Ilievski, M. Mierzejewski, J. Herbrych, and P. Prelovšek, *Spin diffusion in a perturbed isotropic Heisenberg spin chain*, *Phys. Rev. B* **108**, L081115 (2023).

[40] J. Richter and A. Pal, *Anomalous hydrodynamics in a class of scarred frustration-free Hamiltonians*, *Phys. Rev. Research* **4**, L012003 (2022).

[41] J. Richter, O. Lunt, and A. Pal, *Transport and entanglement growth in long-range random Clifford circuits*, *Phys. Rev. Research* **5**, L012031 (2023).

[42] M. Michel, M. Hartmann, J. Gemmer, and G. Mahler, *Fourier's Law confirmed for a class of small quantum systems*, *Eur. Phys. J. B* **34**, 325 (2003).

[43] H. Wichterich, M. J. Henrich, H.-P. Breuer, J. Gemmer, and M. Michel, *Modeling heat transport through completely positive maps*, *Phys. Rev. E* **76**, 031115 (2007).

[44] M. Žnidarič, *Spin Transport in a One-Dimensional Anisotropic Heisenberg Model*, *Phys. Rev. Lett.* **106**, 220601 (2011).

[45] M. Žnidarič, A. Scardicchio, and V. K. Varma, *Diffusive and Subdiffusive Spin Transport in the Ergodic Phase of a Many-Body Localizable System*, *Phys. Rev. Lett.* **117**, 040601 (2016).

[46] T. Prosen and M. Žnidarič, *Matrix product simulations of non-equilibrium steady states of quantum spin chains*, *J. Stat. Mech.* **2009**, P02035 (2009).

[47] F. Verstraete, J. J. García-Ripoll, and J. I. Cirac, *Matrix Product Density Operators: Simulation of Finite-Temperature and Dissipative Systems*, *Phys. Rev. Lett.* **93**, 207204 (2004).

[48] M. Zwolak and G. Vidal, *Mixed-State Dynamics in One-Dimensional Quantum Lattice Systems: A Time-Dependent Superoperator Renormalization Algorithm*, *Phys. Rev. Lett.* **93**, 207205 (2004).

[49] H. Weimer, A. Kshetrimayum, and R. Orús, *Simulation methods for open quantum many-body systems*, *Rev. Mod. Phys.* **93**, 015008 (2021).

[50] Z. Lenarčič, O. Alberton, A. Rosch, and E. Altman, *Critical Behavior near the Many-Body Localization Transition in Driven Open Systems*, *Phys. Rev. Lett.* **125**, 116601 (2020).

[51] P. Prelovšek, S. Nandy, Z. Lenarčič, M. Mierzejewski, and J. Herbrych, *From dissipationless to normal diffusion in the easy-axis Heisenberg spin chain*, *Phys. Rev. B* **106**, 245104 (2022).

[52] R. Steinigeweg, M. Ogiewa, and J. Gemmer, *Equivalence of transport coefficients in bath-induced and dynamical scenarios*, *EPL (Europhys. Lett.)* **87**, 10002 (2009).

[53] M. Žnidarič and M. Ljubotina, *Interaction instability of localization in quasiperiodic systems*, *Proc. Natl. Acad. Sci. USA* **115**, 4595 (2018).

[54] T. Heitmann, J. Richter, J. Herbrych, J. Gemmer, and R. Steinigeweg, *Real-time broadening of bath-induced density profiles from closed-system correlation functions*, *Phys. Rev. E* **108**, 024102 (2023).

[55] A. Purkayastha, S. Sanyal, A. Dhar, and M. Kulkarni, *Anomalous transport in the Aubry-André-Harper model in isolated and open systems*, *Phys. Rev. B* **97**, 174206 (2018).

[56] A. Kundu, A. Dhar, and O. Narayan, *The Green-Kubo formula for heat conduction in open systems*, *J. Stat. Mech.* **2009**, L03001 (2009).

[57] A. Purkayastha, *Classifying transport behavior via current fluctuations in open quantum systems*, *J. Stat. Mech.* **2019**, 043101 (2019).

[58] M. Žnidarič, *Nonequilibrium steady-state Kubo formula: Equality of transport coefficients*, *Phys. Rev. B* **99**, 035143 (2019).

[59] R. Steinigeweg, F. Jin, D. Schmidtke, H. De Raedt, K. Michielsen, and J. Gemmer, *Real-time broadening of nonequilibrium density profiles and the role of the specific initial-state realization*, *Phys. Rev. B* **95**, 035155 (2017).

[60] R. Steinigeweg, H. Wichterich, and J. Gemmer, *Density dynamics from current auto-correlations at finite time- and length-scales*, *EPL (Europhys. Lett.)* **88**, 10004 (2009).

[61] R. Steinigeweg, J. Gemmer, and W. Brenig, *Spin and energy currents in integrable and nonintegrable spin-1/2 chains: A typicality approach to real-time autocorrelations*, *Phys. Rev. B* **91**, 104404 (2015).

[62] R. Steinigeweg and J. Gemmer, *Density dynamics in translationally invariant spin-1/2 chains at high temperatures: A current-autocorrelation approach*, *Phys. Rev. B* **80**, 184402 (2009).

[63] R. Steinigeweg and W. Brenig, *Spin Transport in the XXZ Chain at Finite Temperature and Momentum*, *Phys. Rev. Lett.* **107**, 250602 (2011).

[64] C. Karrasch, J. E. Moore, and F. Heidrich-Meisner, *Real-time and real-space spin and energy dynamics in one-dimensional spin-1/2 systems induced by local quantum quenches at finite temperatures*, *Phys. Rev. B* **89**, 075139 (2014).

[65] See supplemental material for additional notes and numerical data for large coupling γ , strong driving μ , other anisotropies Δ , as well as for open boundary conditions of the system. The supplemental material also contains Refs. [78, 79].

[66] H. De Raedt, F. Jin, M. I. Katsnelson, and K. Michielsen, *Relaxation, thermalization, and Markovian dynamics of two spins coupled to a spin bath*, *Phys. Rev. E* **96**, 053306 (2017).

[67] I. de Vega and D. Alonso, *Dynamics of non-Markovian open quantum systems*, *Rev. Mod. Phys.* **89**, 015001 (2017).

[68] J. Dalibard, Y. Castin, and K. Mølmer, *Wave-function approach to dissipative processes in quantum optics*, *Phys. Rev. Lett.* **68**, 580 (1992).

[69] M. Michel, O. Hess, H. Wichterich, and J. Gemmer, *Transport in open spin chains: A Monte Carlo wave-function approach*, *Phys. Rev. B* **77**, 104303 (2008).

[70] J. Gemmer, M. Michel, and G. Mahler, *Quantum Thermodynamics*, Lecture Notes in Physics, Vol. 657

(Springer Berlin Heidelberg, 2004).

[71] S. Goldstein, J. L. Lebowitz, R. Tumulka, and N. Zanghì, *Canonical Typicality*, Phys. Rev. Lett. **96**, 050403 (2006).

[72] S. Popescu, A. J. Short, and A. Winter, *Entanglement and the foundations of statistical mechanics*, Nat. Phys. **2**, 754 (2006).

[73] P. Reimann, *Typicality for Generalized Microcanonical Ensembles*, Phys. Rev. Lett. **99**, 160404 (2007).

[74] C. Bartsch and J. Gemmer, *Dynamical Typicality of Quantum Expectation Values*, Phys. Rev. Lett. **102**, 110403 (2009).

[75] B. N. Balz, J. Richter, J. Gemmer, R. Steinigeweg, and P. Reimann, in *Thermodynamics in the Quantum Regime* (Springer, Cham, 2018) pp. 413–433.

[76] $D/J \approx 0.023471/0.023653 \approx 0.99$.

[77] Jülich Supercomputing Centre, *JUWELS Cluster and Booster: Exascale Pathfinder with Modular Supercomputing Architecture at Jülich Supercomputing Centre*, JLSRF **7**, A138 (2021).

[78] P. Fendley, *Strong zero modes and eigenstate phase transitions in the XYZ/interacting Majorana chain*, J. Phys. A **49**, 30LT01 (2016).

[79] J. Kemp, N. Y. Yao, C. R. Laumann, and P. Fendley, *Long coherence times for edge spins*, J. Stat. Mech. **2017**, 063105 (2017).

[80] $D/J \approx 0.020230/0.033511 \approx 0.60$.

[81] $D/J \approx 0.007809/0.012362 \approx 0.63$.

**Supplemental material of
“Spin-1/2 XXZ chain coupled to two Lindblad baths:
Constructing nonequilibrium steady states from equilibrium correlation functions”**

Tjark Heitmann ^{1,*} Jonas Richter ^{2,3} Fengping Jin ⁴ Sourav Nandy, ⁵ Zala Lenarčič ⁵ Jacek Herbrych ⁶ Kristel Michelsen ⁴ Hans De Raedt ⁷ Jochen Gemmer, ¹ and Robin Steinigeweg ^{1,†}

¹Department of Mathematics/Computer Science/Physics,
University of Osnabrück, D-49076 Osnabrück, Germany

²Department of Physics, Stanford University, Stanford, California 94305, USA

³Institut für Theoretische Physik, Leibniz Universität Hannover, 30167 Hannover, Germany

⁴Institute for Advanced Simulation, Jülich Supercomputing Centre,
Forschungszentrum Jülich, D-52425 Jülich, Germany

⁵Jožef Stefan Institute, SI-1000 Ljubljana, Slovenia

⁶Wroclaw University of Science and Technology, 50-370 Wroclaw, Poland

⁷Zernike Institute for Advanced Materials, University of Groningen, NL-9747 AG Groningen, Netherlands

(Dated: November 28, 2023)

DETAILS ON THE DERIVATION OF THE THEORETICAL PREDICTION

In this section, we are going to sketch the derivation of our theoretical prediction given in Eq. (17) of the main text, which is an extension of the derivation in Ref. [54], where only a single Lindblad bath was considered, instead of the two baths treated here.

To this end, let us for the moment consider a simple scenario featuring a jump with the Lindblad operator L_1 immediately at some time t , say $t = 0$. Then,

$$|\psi(0)\rangle \rightarrow |\psi'\rangle \propto L_1 |\psi(0)\rangle. \quad (\text{S1})$$

For a random initial state $|\psi(0)\rangle$, as given in Eq. (16), this jump results in a random superposition over a subset of pure states with a spin-up at site B_1 , which mimics $\rho(0) \propto \mathbb{1} + S_{B_1}^z$.

At weak driving $\mu \ll 1$, the subsequent deterministic evolution before the next jump reads

$$d_r(t) \equiv \frac{\langle \psi'(t) | S_r^z | \psi'(t) \rangle}{\| |\psi'(t)\rangle \|^2} \approx \langle \psi' | e^{iHt} S_r^z e^{-iHt} | \psi' \rangle, \quad (\text{S2})$$

cf. Eq. (12) of the main text. Now, using the concept of typicality, Eq. (S2) can be rewritten as

$$\frac{d_r(t)}{2} \approx \langle S_r^z(t) S_{B_1}^z(0) \rangle_{\text{eq}} \quad (\text{S3})$$

with $S_r^z(t) = e^{iHt} S_r^z e^{-iHt}$ and $\langle \bullet \rangle_{\text{eq}} = \text{tr}[\bullet]/2^N$ denoting the infinite-temperature ensemble [59]. Analogously, one can obtain such a relation for the other possible jumps with the Lindblad operators L_j , which then involve either $\langle S_r^z(t) S_{B_1}^z(0) \rangle_{\text{eq}}$ or $\langle S_r^z(t) S_{B_2}^z(0) \rangle_{\text{eq}}$. Note that in the derivation of Eq. (S3), we used the facts that

$S_r^z = n_r - \mathbb{1}/2$, $(n_r)^2 = n_r$, and $\text{tr}[S_r^z(t)] = 0$, see e.g., Ref. [24] for more details.

For the above homogeneous initial state $|\psi(0)\rangle$, the jump probabilities according to Eq. (14) are simply given by $p_j = \alpha_j/4\gamma$. Consequently, averaging over all 4 jumps possibilities,

$$\begin{aligned} \bar{d}_r(t) &= (p_1 - p_2) \langle S_r^z(t) S_{B_1}^z(0) \rangle_{\text{eq}} \\ &\quad + (p_3 - p_4) \langle S_r^z(t) S_{B_2}^z(0) \rangle_{\text{eq}} \end{aligned} \quad (\text{S4})$$

yields the theoretical prediction

$$\bar{d}_r(t) = \mu \langle S_r^z(t) S_{B_1}^z(0) \rangle_{\text{eq}} - \mu \langle S_r^z(t) S_{B_2}^z(0) \rangle_{\text{eq}} \quad (\text{S5})$$

for the time evolution after the first and before the second jump.

Let us consider a second jump at a later time τ . The corresponding jump probabilities p_j can then be derived based on typicality arguments. To this end, we assume a random pure state $|\psi(\tau - 0^+)\rangle$ right before the jump with $\bar{d}_{B_1}(\tau - 0^+) \neq 0$ and $\bar{d}_{B_2}(\tau - 0^+) \neq 0$. Then, due to the symmetry

$$\bar{d}_{B_1}(\tau - 0^+) = -\bar{d}_{B_2}(\tau - 0^+) \quad (\text{S6})$$

we have

$$y_1 = \|L_1|\psi(\tau - 0^+)\rangle\|^2 = \frac{1}{2} - \bar{d}_{B_1}(\tau - 0^+) \quad (\text{S7})$$

$$y_2 = \|L_2|\psi(\tau - 0^+)\rangle\|^2 = \frac{1}{2} + \bar{d}_{B_1}(\tau - 0^+) \quad (\text{S8})$$

$$y_3 = \|L_3|\psi(\tau - 0^+)\rangle\|^2 = \frac{1}{2} - \bar{d}_{B_2}(\tau - 0^+) = y_2 \quad (\text{S9})$$

$$y_4 = \|L_4|\psi(\tau - 0^+)\rangle\|^2 = \frac{1}{2} + \bar{d}_{B_2}(\tau - 0^+) = y_1 \quad (\text{S10})$$

with $y_1 + y_2 + y_3 + y_4 = 1$. Thus, the jump probabilities read

$$p_1 = p_4 = \frac{1}{2} \frac{(1 + \mu)y_1}{(1 + \mu)y_1 + (1 - \mu)y_2} \quad (\text{S11})$$

$$p_2 = p_3 = \frac{1}{2} \frac{(1 - \mu)y_1}{(1 + \mu)y_1 + (1 - \mu)y_2} \quad (\text{S12})$$

* tjark.heitmann@uos.de

† rsteinig@uos.de

with $p_1 + p_2 + p_3 + p_4 = 1$. A straightforward calculation yields

$$p_1 - p_2 = p_4 - p_3 = \frac{\mu - 2\bar{d}_{B_1}(\tau - 0^+)}{2 - 4\mu \bar{d}_{B_1}(\tau - 0^+)} . \quad (S13)$$

Using this expression, we can define the amplitude

$$A_\tau = \frac{(p_1 - p_2) - \bar{d}_{B_1}(\tau - 0^+)}{\mu} , \quad (S14)$$

to incorporate both the probabilities for the next jump as well as the fact that some magnetization is already induced at the bath site. With this, we can eventually formulate a theoretical prediction for the deterministic evolution after the second jump, in analogy to the case of a single Lindblad bath [54]. This prediction reads

$$\bar{d}_r(t) = \mu \mathcal{C}_r(t) + 2\mu A_\tau \Theta(t - \tau) \mathcal{C}_r(t - \tau) \quad (S15)$$

with the Heavyside function $\Theta(t)$ and the abbreviation

$$\mathcal{C}_r(t) = \langle S_r^z(t) S_{B_1}^z(0) \rangle_{\text{eq}} - \langle S_r^z(t) S_{B_2}^z(0) \rangle_{\text{eq}} . \quad (S16)$$

Reiterating this procedure finally yields a generalization of Eq. (S15) to a sequence of jump times τ_j ,

$$\bar{d}_r(t) = 2\mu \sum_j A_j \Theta(t - \tau_j) \mathcal{C}_r(t - \tau_j) , \quad (S17)$$

i.e., Eq. (17) in the main text.

As discussed in Ref. [54], the central assumption within the above derivation is that the system has sufficient time to equilibrate between two jumps or, in other words, the magnetization injected at the contact sites has to spread over some region of the system. This requirement means that, in addition to a weak driving μ , one has to choose a small coupling γ . Still, it might happen that even for a small coupling the equilibration process is hampered, as it is the case for open boundary conditions in certain models and parameter regimes, see the discussion below for more details.

PERFECT DIFFUSION

As mentioned in the main text, we attribute differences between diffusion constants in open and closed systems to finite-size effects at long times, where the steady state is established. To support this, it is instructive to consider the idealized assumption of perfect diffusion in the closed system. In this case, which has no finite-size effects at any time, the equilibrium correlation functions take on the simple form [9]

$$\langle S_r^z(t) S_{r'}^z(0) \rangle_{\text{eq}} = \frac{1}{4} e^{-2D_{\text{closed}} t} \mathcal{I}_{r-r'}(2D_{\text{closed}} t) , \quad (S18)$$

where $\mathcal{I}_r(t)$ is the modified Bessel function of the first kind and of the order r . Choosing $D_{\text{closed}}/J = 0.6$, we

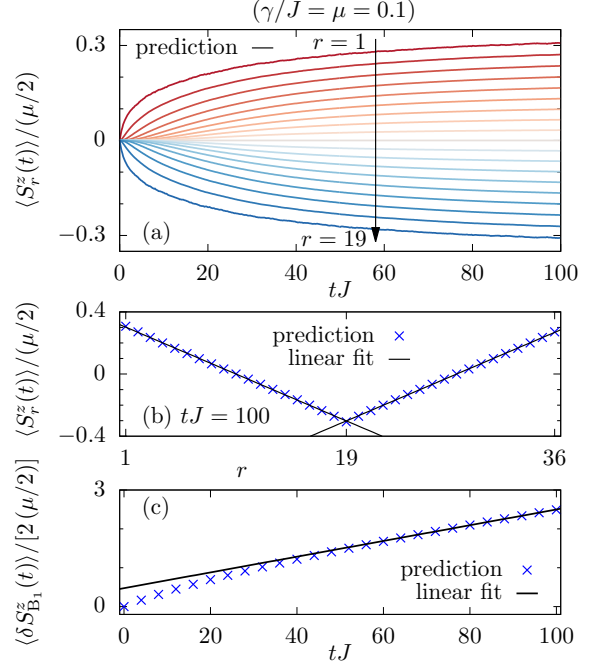


FIG. S1. Prediction under the idealized assumption that the closed system is perfectly diffusive with a diffusion constant $D/J = 0.6$. In the open system, the corresponding diffusion constant obtained from the steady state is $D/J \approx 0.60$ [80].

show our prediction for the open system in Fig. S1. Indeed, using the relationship $D = -\langle j_r \rangle / \nabla \langle S_r \rangle$, we find a corresponding diffusion constant $D/J \approx 0.60$ in the steady state [80]. Thus, for perfectly diffusive behavior without finite-size effects, the steady state yields the same transport coefficient as the equilibrium correlation function (in contrast to the realistic case discussed in the context of Fig. 3 in the main text).

Furthermore, as already discussed in the main text, it is possible to calculate $D(t)$ already at finite times before the steady state is established, via

$$D(t) = \frac{\partial_t \langle S_r^z(t) \rangle}{\nabla^2 \langle S_r^z(t) \rangle} \quad (S19)$$

with

$$\nabla^2 \langle S_r^z(t) \rangle = \langle S_{r-1}^z(t) \rangle - 2\langle S_r^z(t) \rangle + \langle S_{r+1}^z(t) \rangle , \quad (S20)$$

which is just the diffusion equation for a lattice in one spatial dimension. Evaluating this expression for, e.g., site $r = 9$ and time $tJ = 25$ for the perfectly diffusive data in Fig. S1, we obtain the value

$$D/J \approx \frac{(0.012748 - 0.012062)/1}{0.025282 - 2 \cdot 0.012062 + 0} \approx 0.59 , \quad (S21)$$

which is again in good agreement with D_{closed} .

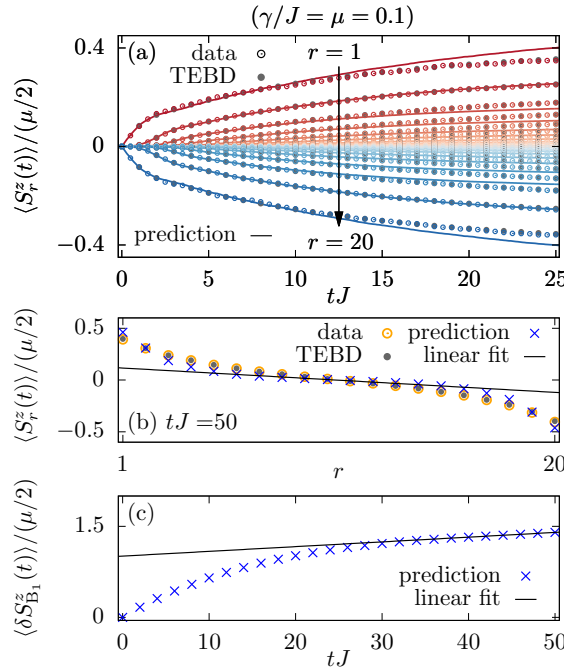


FIG. S2. [(a) and (b)] Analogous to Fig. 2 of the main text, but now with open boundary conditions and bath sites $B_1 = 1$ and $B_2 = N$, where $N = 20$. Numerical results obtained by stochastic unraveling (data) are compared to our prediction based on equilibrium correlation functions [cf. Eq. (20)]. Furthermore, we show data obtained by solving the Lindblad equation using a time-evolving block decimation (TEBD) approach, which are in perfect agreement with the stochastic unraveling. The diffusion constant extracted from the steady state is $D/J \approx 0.63$ [81].

OPEN BOUNDARIES AND COMPARISON WITH TEBD SIMULATIONS

So far, we have focused on systems with periodic boundary conditions, which are the natural choice for closed systems, whereas state-of-the-art matrix product state approaches to open systems commonly rely on open boundary conditions with Lindblad driving at the systems' edges.

In Fig. S2, we show a comparison between our theoretical prediction (20) and full stochastic unraveling, similar to Fig. 2 in the main text, but now for a XXZ chain with open boundaries, where the two baths are placed at the ends of the chain, $B_1 = 1$ and $B_2 = N$. As shown in Fig. S2(a), the time evolution of the local magnetization $\langle S_r^z(t) \rangle$ is well captured by the prediction (20), though deviations start to appear at times $tJ \gtrsim 20$. These slight deviations might be caused by the fact that the equilibrium correlation functions can exhibit unusual behavior in the case of open boundary conditions. In particular, $\langle S_{B_1}^z(t) S_{B_1}^z(0) \rangle$ and $\langle S_{B_2}^z(t) S_{B_2}^z(0) \rangle$ do not fully decay for any $\Delta > 1$ in the case of open boundary conditions due to the presence of a strong zero mode, where the edge spins retain memory of their initial conditions for very

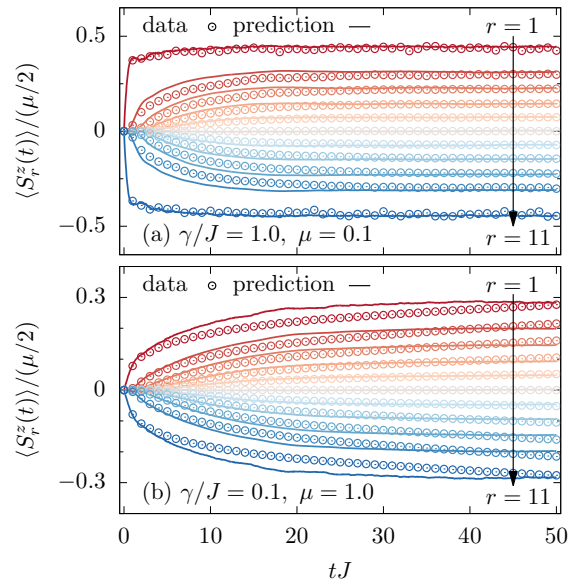


FIG. S3. Time evolution of the local magnetizations $\langle S_r^z(t) \rangle$ for the model parameters in Fig. 2, but for the cases of (a) large coupling $\gamma/J = 1$ ($\mu = 0.1$) and (b) strong driving $\mu = 1$ ($\gamma/J = 0.1$). As before, the derived prediction is compared to stochastic unraveling (data).

long times [78, 79].

In addition to our prediction (20) and the stochastic unraveling, we include in Fig. S2 numerical data obtained by a state-of-the-art matrix product state implementation based on time-evolving block decimation (TEBD) with time step $dtJ = 0.05$ and bond dimension $\chi = 128$. Importantly, we find that this TEBD data is in perfect agreement with the results from stochastic unraveling.

The convincing agreement between TEBD, stochastic unraveling, and our theoretical prediction is further highlighted in Fig. S2(b), where the site dependence of the profile $\langle S_r^z(t) \rangle$ is shown for time $tJ = 50$. Moreover, we find that this profile is well described by a linear function in the bulk, far away from the bath contacts. The injected magnetization $\langle \delta S_{B_1}^z(t) \rangle$ is shown in Fig. S2(c). The diffusion constant in the open system is again given by the ratio of the slopes in Figs. S2(b) and S2(c). This way, we find the value $D/J \approx 0.63$ in very good agreement with the value $D/J \approx 0.6$ in the closed system.

INJECTED MAGNETIZATION

The first Lindblad bath injects magnetization at the corresponding contact site $r = B_1$. This magnetization can also be predicted and written as

$$\langle \delta S_{B_1}^z(t) \rangle \approx \frac{1}{T_{\max}} \sum_{T=1}^{T_{\max}} \delta d_{B_1, T}(t) \quad (\text{S22})$$

with

$$\frac{\delta d_{B_1,T}(t)}{2\mu} = \sum_j A_j \Theta(t - \tau_j) \langle [S_{B_1}^z(0)]^2 \rangle, \quad (S23)$$

cf. Eq. (17). This magnetization can then be related to the local currents, which are all the same in the steady state, i.e.,

$$\langle j_r \rangle = \langle j_{r'} \rangle, \quad B_1 \leq r, r' \leq B_2. \quad (S24)$$

Thus, it is sufficient to know $\langle j_{B_1} \rangle$, which follows from the injected magnetization via

$$\langle j_{B_1} \rangle = \frac{d}{dt} \frac{\langle \delta S_{B_1}^z(t) \rangle}{2}, \quad (S25)$$

where the factor 1/2 takes into account that the injected magnetization can flow to the left and to the right of this bath, due to periodic boundary conditions. By the use of this expression, we find that, for the case discussed in Fig. 2, $\langle j_r \rangle/J \approx 0.0028$.

For comparison, we can calculate the local currents for the same model within the stochastic unraveling as

$$\langle j_r \rangle \approx \frac{1}{T_{\max}} \sum_{T=1}^{T_{\max}} \frac{\langle \psi_T(t) | j_r | \psi_T(t) \rangle}{\| \psi_T(t) \|^2} \quad (S26)$$

for $\mathcal{O}(10^4)$ trajectories. For long times $tJ \gtrsim 30$, where the steady state is established, we find a corresponding value of $\langle j_r \rangle/J \approx 0.003$, which is close to the predicted one above.

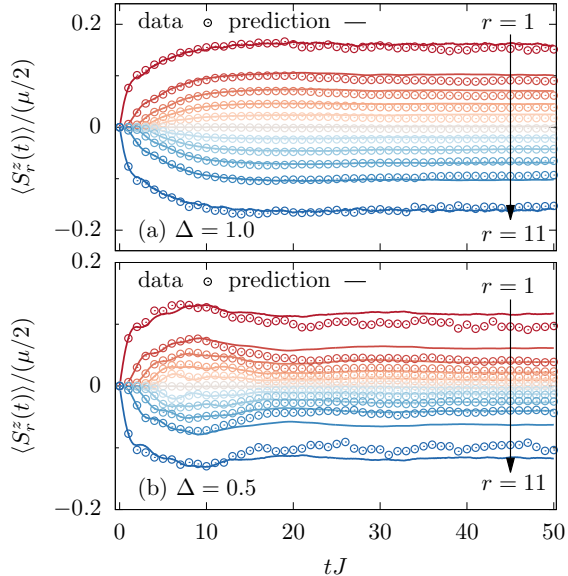


FIG. S4. Time evolution of the local magnetizations $\langle S_r^z(t) \rangle$ for the model parameters in Fig. 2, but for the anisotropies (a) $\Delta = 1.0$ and (b) $\Delta = 0.5$. As before, the derived prediction is compared to stochastic unraveling (data).

LARGE COUPLING / STRONG DRIVING

In the main text, we have focused on the case of small coupling $\gamma/J = 0.1$ and weak driving $\mu = 0.1$, where we have found a convincing agreement between the derived prediction and exact numerics in Fig. 2. To illustrate that deviations occur for larger coupling or stronger driving, we depict a corresponding comparison for (a) $\gamma/J = 1$ ($\mu = 0.1$) and (b) $\mu = 1$ ($\gamma/J = 0.1$) in Fig. S3. In both cases (a) and (b), deviations are visible already at finite times before the steady state is reached. Interestingly, in the case (a) of strong coupling, the overall agreement is still satisfactory and the profile in the steady state is predicted accurately.

OTHER ANISOTROPIES

In Fig. 2 of the main text, we have provided a comparison of the magnetization dynamics for anisotropy $\Delta = 1.5$. Complementarily, we show a comparison for anisotropies (a) $\Delta = 1.0$ and (b) $\Delta = 0.5$ in Fig. S4. For the case of $\Delta = 1.0$, we again find a convincing agreement. While for the case of $\Delta = 0.5$ the overall behavior of prediction and numerics is still similar, deviations are visible at long time scales. These deviations reflect that the prediction is not exact in a mathematical sense but involves physical assumptions (such as, e.g., on the equilibration properties of the involved equilibrium correlation functions) which may not hold perfectly in any given situation.